Research Square

Preprints are preliminary reports that have not undergone peer review.
They should not be considered conclusive, used to inform clinical practice,
or referenced by the media as validated information.

MTAP-Deficiency Identifies a Myofibroblastic and Immune-Attenuated Tumor Microenvironment Subtype in Pancreatic Ductal Adenocarcinoma

Julian Karlbauer

julian.karlbauer@fau.de

University Hospital Cologne

Karl Knipper
University Hospital Cologne

Tillmann Bedau
University Hospital Cologne

Hans Schloesser
University Hospital Cologne

Michael Thomas
University Hospital Cologne

Reinhard Buettner
University Hospital Cologne

Christiane Bruns
University Hospital Cologne

Felix C. Popp
University Hospital Cologne

Su Ir Lyu
University Hospital Cologne

Alexander Quaas
University Hospital Cologne

Article

Keywords: MTAP immunohistochemistry, pancreatic ductal adenocarcinoma, CDKN2A deletion, cancer-associated fibroblasts, tumor microenvironment

Posted Date: August 18th, 2026

DOI: https://doi.org/10.21203/rs.3.rs-10656530/v1

License: This work is licensed under a Creative Commons Attribution 4.0 International License.
Read Full License

Additional Declarations: No competing interests reported.

Abstract

MTAP protein loss is a surrogate for homozygous CDKN2A deletion and marks a therapeutically actionable, PRMT5-dependent subgroup of pancreatic ductal adenocarcinoma (PDAC), but its tumor microenvironment (TME) remains uncharacterized. In 370 surgically resected PDAC from the prospective multicentric PANCALYZE cohort, MTAP status was determined by immunohistochemistry and confirmed by CDKN2A fluorescence in situ hybridization in MTAP-deficient cases. Immune and stromal cancer-associated fibroblast (CAF) markers were quantified by digital image analysis. Subtype-associated markers were scored by pathologists. MTAP loss occurred in 39.5% of PDAC and showed complete concordance with homozygous CDKN2A deletion. Patients with MTAP deficiency were significantly younger and at higher lymph-node stage. MTAP-loss PDAC displayed a distinct stromal and immune profile, with higher SMA + and FAP + and lower PDGFRβ + CAFs and reduced natural killer-cell and plasma-cell infiltration, not explained by basal-like subtype. MTAP status was not prognostic (median overall survival [OS] 22.0 months in both groups). Within MTAP-deficient PDAC, Claudin 18.2 positivity was associated with longer OS ($p = 0.025$), whereas high γH2AX ($p = 0.003$) and high M2-like macrophage infiltration ($p = 0.007$) were associated with shorter OS. Only high γH2AX remained independent on multivariable analysis ($p = 0.028$). MTAP loss thus marks a myofibroblastic, immune-attenuated TME, warranting consideration in translational studies of MTAP-directed therapies.

Introduction

Pancreatic ductal adenocarcinoma (PDAC) is one of the most lethal solid malignancies and is characterized by aggressive tumor biology, early metastasis, and limited therapeutic options, resulting in a persistently poor overall survival despite advances in surgical and systemic treatment strategies [1, 2]. The molecular landscape of PDAC is dominated by recurrent genetic alterations affecting *KRAS, TP53, SMAD4*, and *CDKN2A*, the latter representing one of the most frequently inactivated tumor suppressor genes in PDAC and playing a central role in cell cycle regulation and tumor progression [2–4]. The gene encoding 5'-methylthioadenosine phosphorylase (MTAP) is located on chromosome 9p21.3 in close genomic proximity to *CDKN2A*. Due to this genomic co-localization, homozygous deletions of *CDKN2A* frequently extend to the adjacent MTAP locus, resulting in concomitant loss of MTAP expression [5, 6]. MTAP is a key enzyme in the methionine and adenine salvage pathway and loss of MTAP function leads to intracellular accumulation of methylthioadenosine (MTA), which inhibits protein arginine methyltransferase 5 (PRMT5), an essential epigenetic regulator involved in RNA splicing, gene expression, and cell cycle control [7, 8]. As a result, MTAP-deficient tumor cells develop a specific metabolic dependency on PRMT5. Consequently, MTA-cooperative PRMT5 inhibitors have shown selective activity in MTAP-deleted tumors and clinical trials including a dedicated first-line phase 2/3 trial in MTAP-deleted metastatic PDAC are ongoing (navlimetostat; MountainTAP-30, NCT07076121) [9–12]. Reliable identification of MTAP-deficient tumors is therefore of growing clinical importance. Because MTAP loss closely mirrors homozygous CDKN2A deletion, MTAP IHC has been adopted as a practical surrogate for 9p21/CDKN2A loss in several tumor types, including central nervous system tumors and pleural mesothelioma [6, 13, 14]. In PDAC, other groups have reported generally high but not uniform

concordance between MTAP IHC and CDKN2A status [15], with occasional discordance [16]. Within our own multi-entity series, FISH validation was performed only in esophageal adenocarcinoma, so a dedicated correlation of MTAP IHC with CDKN2A FISH in this PDAC cohort had not previously been established [17]. While the diagnostic implications of MTAP loss are increasingly recognized, far less is known about the biology of MTAP-deficient PDAC. PDAC is characterized by an exceptionally dense, immunosuppressive TME in which heterogeneous CAFs — spanning myofibroblastic and inflammatory phenotypes marked by α-smooth muscle actin (SMA), fibroblast activation protein (FAP), platelet-derived growth factor receptor-β (PDGFRβ) and periostin — and a variable immune infiltrate together shape progression, therapy response and prognosis [18–21]. Notably, 9p21/MTAP loss has been linked to a cold, lymphocyte-poor immune microenvironment and to primary resistance to immune-checkpoint inhibition, an effect attributed specifically to MTA-mediated impairment of lymphocyte function rather than to CDKN2A loss [22, 23]. Whether MTAP-deficient PDAC exhibits a distinct stromal and immune phenotype, whether such a phenotype is simply a reflection of established subtype-associated features such as basal-like differentiation, and how it relates to other subtype-associated markers such as Claudin 18.2 [24] and γH2AX [25], has not been comprehensively characterized [26, 27].

We therefore studied 370 surgically resected PDAC from the prospective multicentric PANCALYZE cohort. Using an immunohistochemistry-first, FISH-confirmatory workflow, we defined MTAP-deficient tumors by MTAP IHC and confirmed homozygous CDKN2A deletion by FISH in these cases, thereby establishing the positive predictive value of MTAP loss for CDKN2A deletion. We then characterized the stromal and immune microenvironment of the MTAP-deficient tumors, in comparison with MTAP-intact PDAC, combining quantitative digital image analysis with pathologist-based scoring.

Results

Cohort and definition of the MTAP-deficient subgroup

A total of **370 patients** with surgically resected PDAC were included. **MTAP loss of expression was observed in 146 cases (39.5%)**, while **224 tumors (60.5%) showed intact MTAP expression**. To robustly define the MTAP-deficient subgroup for the subsequent microenvironmental analyses, all MTAP-deficient cases were examined by confirmatory CDKN2A FISH, which demonstrated homozygous CDKN2A deletion in all 146 cases. The region-matched IHC–FISH correspondence is shown for a representative case in **Figure 1** and for an additional case in **Supplementary Figure S1**, and a selection of re-evaluated cases on whole sections is shown in **Supplementary Figure S3**. As FISH was applied only as a confirmatory step in the IHC-defined MTAP-loss cases and not in MTAP-retained cases, this reflects the positive predictive value of MTAP loss for CDKN2A homozygous deletion.

MTAP loss is associated with an SMA/FAP-high, PDGFRβ-low stromal marker profile and reduced NK- and plasma-cell infiltration

Quantitative digital image analysis revealed significant differences between MTAP-deficient and MTAP-intact PDAC (Figure 2; Supplementary Table S3). Among CAF markers, MTAP-deficient tumors showed

lower PDGFRβ+ stroma (39.3% vs. 57.1%; p<0.001), higher FAP+ (57.2% vs. 45.5%; p=0.028) and higher SMA+ (58.5% vs. 46.4%; p=0.049) CAFs, consistent with an SMA/FAP-high, PDGFRβ-low stromal marker profile. Periostin did not differ. Within the inflammatory compartment, MTAP-deficient tumors exhibited lower CD56+ natural killer-cell (42.4% vs. 55.0%; p=0.019) and CD38+ plasma-cell (41.5% vs. 53.6%; p=0.049) infiltration, whereas CD3+ T cells, CD20+ B cells, CD66b+ neutrophils, CD117+ mast cells and CD163+ macrophages did not differ significantly. These findings indicate a selective immune attenuation rather than global immune depletion. MTAP status was not significantly associated with basal-like differentiation, nor with Claudin 18.2 or γH2AX in the overall cohort. Representative single-core immunohistochemistry for MTAP and three of the significantly altered markers (FAP, PDGFRβ, CD56) is shown in Supplementary Figure S2.

MTAP status alone is not prognostic

Overall survival analysis included all 370 patients (244 deaths; 126 censored, 34.1%). There was no significant difference in OS between MTAP-deficient and MTAP-intact PDAC (median OS 22.0 months in both groups; mean 31.0 [95% CI 25.0–36.9] vs. 36.0 months [95% CI 30.8–41.2]) (Figure 3A).

Clinicopathological characteristics according to MTAP status

Patients with MTAP-deficient tumors were significantly younger (aged <65 years: 42.5% vs. 29.5%; p=0.010) and had a higher lymph-node stage (p=0.045). Sex, primary tumor stage, resection status, perineural invasion, lymphatic invasion, blood invasion, tumor grading and neoadjuvant therapy did not differ significantly (Table 1).

Outcome within MTAP-deficient PDAC

Because MTAP-deficient PDAC represents the subgroup most relevant for MTAP-directed therapeutic strategies, we next examined which microenvironmental and subtype-associated markers were associated with outcome within this group. Three markers were significantly associated with OS: Claudin 18.2 positivity with longer survival (30.0 vs. 15.0 months; p=0.025), and high γH2AX (14.0 vs. 26.0 months; p=0.003) and high CD163+ macrophage infiltration (18.0 vs. 26.0 months; p=0.007) with shorter survival (Table 2, Figure 3C–E). A broader panel (CD4, CD8, CD68, MUM1, ERG, MCT, Tenascin, BRM, BRG1, FOXP3; Supplementary Table S1) showed only a non-significant trend toward shorter OS for low FOXP3 (17.0 vs. 26.0 months; p=0.054). The remaining markers were not associated with OS.

To determine which of these markers was independent of the others and of standard clinicopathological factors, we constructed a multivariable Cox model including all variables with p<0.20 on univariable analysis. High γH2AX expression was the only independent predictor of worse OS (HR 1.97, 95% CI 1.08–3.62; p=0.028). None of the other variables (CD163, FAP, FOXP3, age, neoadjuvant therapy, pT, pN, R category, blood invasion) retained significance (Table 3).

Discussion

In this study of 370 surgically resected PDAC, MTAP loss marked a biologically distinct subgroup characterized by an SMA/FAP-high, PDGFRβ-low CAF marker profile and selectively reduced NK-cell and plasma-cell infiltration. This microenvironmental phenotype was not explained by basal-like tumor cell differentiation. MTAP status itself was not prognostic, whereas outcome within MTAP-deficient tumors was associated with γH2AX-defined DNA-damage response and selected microenvironmental markers.

The stromal shift we observed — lower PDGFRβ + stroma with higher FAP + and SMA+ CAFs — is best interpreted in the context of CAF heterogeneity. CAFs in PDAC are heterogeneous and are commonly grouped into myofibroblastic CAFs, inflammatory CAFs, and antigen-presenting CAFs, with myofibroblastic CAFs characterized by high SMA expression and linked to extracellular matrix production, tumor stiffness, therapy resistance, tumor progression, and immune evasion [18–20]. Against this background, our parallel gain of SMA and FAP points to the activated, myofibroblastic end of this spectrum — though not to a pure myCAF expansion. The lower PDGFRβ signal does not contradict this, as SMA, FAP and PDGFRβ do not mark one uniform cell type. Additionally, unlike SMA, PDGFRβ is expressed broadly across CAF states and perivascular cells rather than being myCAF-specific.

Regarding the immune compartment, our findings likewise point to a selective rather than global shift: MTAP-deficient tumors showed lower CD56 + natural-killer-cell and CD38 + plasma-cell infiltration, without significant changes in CD3 + T cells, CD20 + B cells, CD66b+ tumor-associated neutrophils, CD117 + mast cells or CD163+ (M2-like) macrophages. Rather than a global loss of immune cells, this reflects a selective reduction of cytotoxic and terminally differentiated effector populations which—together with the SMA/FAP-high, PDGFRβ-low stroma—resembles the activated-stroma phenotype associated with low immune infiltration and poor prognosis in PDAC [37]. The reduced NK-cell infiltration is concordant with reports that 9p21/MTAP loss produces a lymphocyte-poor, checkpoint-inhibitor–resistant milieu through MTA-mediated impairment of lymphocyte function rather than through CDKN2A loss [22, 23]. Nevertheless, in our cohort, the T- and B-cell densities were preserved, indicating a more selective attenuation than the globally cold phenotype described in those pan-cancer studies.

A recently published AACR conference abstract by Bady et al. reported a MTAP-stratified PDAC tissue-microarray study (n = 378) in which they found higher CD68 + macrophage density in MTAP-loss PDAC tumors, predominantly in the stroma [38]. Importantly, this signal was carried by the **total** CD68 + macrophage compartment, whereas the CD163 + M2-like subset we assessed did not differ. A comparable macrophage increase, alongside lower B- and T-cell fractions was seen at the transcriptomic level in the pancreatic subset (n = 11,217) of a large sequencing-based analysis of MTAP-deleted gastrointestinal cancers reported in a conference abstract [39]. Across these datasets, stromal and myeloid-oriented remodeling is the most consistent correlate of MTAP loss in PDAC, whereas the cellular specificity of the accompanying lymphoid attenuation differs between tissue- and transcriptome-based studies.

Our whole-cohort CAF findings build on our previous PANCALYZE report, which established high SMA expression as an independent adverse prognostic factor in resected PDAC [30]. We did not re-test SMA

prognosis here. Instead, we show that MTAP loss is enriched for an overlapping SMA-high/FAP-high, PDGFRβ-low stromal marker profile.

We next related the MTAP-associated microenvironment to basal-like differentiation, which we had previously linked to a stroma-rich, plasma-cell-poor phenotype in the same cohort [26]. Although myofibroblastic CAF activation and basal-like tumor biology are generally coupled in PDAC [40], MTAP loss in our cohort was not associated with CK6/CK5/6-defined basal-like tumor cell differentiation and its stromal and immune profile overlapped only partly with the previously reported basal-like-associated profile (shared: higher SMA and lower plasma-cell infiltration; distinct: higher FAP, lower PDGFRβ and lower NK-cell infiltration). Thus, MTAP loss does not appear to be merely a surrogate for basal-like differentiation. Rather, the MTAP-associated stromal shift can occur without a corresponding basal-like epithelial phenotype. As this interpretation is based on marker-level associations rather than formal molecular subtyping, it requires validation in subtype-stratified analyses but is consistent with the concept that tumor-intrinsic and stromal PDAC subtypes provide partly independent prognostic information [41, 42].

Clinically, MTAP-deficient tumors in our study arose in younger patients and at a higher lymph-node stage, in line with 9p21/CDKN2A–MTAP loss marking a biologically more aggressive disease. Despite the distinct biological phenotype associated with MTAP loss, MTAP status itself was not associated with survival, in keeping with our earlier multi-entity analysis [17] and with genomic series reporting no consistent survival association of MTAP loss in this entity [43, 44]. Within the MTAP-deficient subgroup, however, outcome varied with several microenvironmental and subtype-associated markers — each of which stratified survival within the subgroup while showing no significant association with MTAP status across the whole cohort (Table 2). This dissociation indicates that these markers capture prognostically relevant heterogeneity *within* MTAP-deficient PDAC rather than distinguishing features of MTAP-loss itself. Claudin 18.2 positivity, a feature of the classical, better-differentiated phenotype, was associated with longer survival, extending the favorable whole-cohort prognostic role of Claudin 18.2 we previously reported [31] to this molecularly defined subset. Conversely, high γH2AX identified the poorest-outcome subset within MTAP-deficient tumors and was the only factor to remain independent on multivariable analysis — directionally concordant with our previous whole-cohort report [33] and consistent with its established role as a marker of the DNA-damage response [25]. High CD163 + macrophage infiltration was likewise adverse, though only on univariable analysis, in line with the established adverse role of CD163 + M2-like macrophages in PDAC [45] and as discussed above.

These observations have potential clinical relevance. MTAP-deficient PDAC is an emerging target for MTA-cooperative PRMT5 inhibitors [7, 9–11, 46], which have shown activity in MTAP-deleted solid tumors including PDAC (phase 1 CA240-0007: objective response rate 17% among evaluable PDAC patients, n = 35 [12]) and are now being tested in a dedicated first-line phase 2/3 trial in MTAP-deleted metastatic PDAC (navlimetostat/BMS-986504; MountainTAP-30, NCT07076121) [47], with related trials in other MTAP-deleted entities [48] and rational combinations such as concurrent KRAS inhibition under investigation [49]. Our data do not establish a predictive biomarker for response to these agents. They

do suggest, however, that MTAP-deficient PDAC should not be viewed only as a tumor-cell-intrinsic metabolic subgroup: it is accompanied by a distinct stromal and immune marker profile. Because single-agent immune-checkpoint inhibition is largely ineffective in unselected PDAC [50], the myofibroblastic, stroma-rich and selectively immune-attenuated phenotype of MTAP-deficient tumors may argue for combination and stroma- or immune-directed strategies, and TME composition could help refine patient selection within this subgroup and inform rational combination approaches.

In our cohort, all MTAP-deficient cases were confirmed to harbor homozygous CDKN2A deletion by FISH, using an IHC-first, FISH-confirmatory workflow with re-evaluation of equivocal cases on large-area whole sections (Supplementary Figure S3). Because FISH was applied only as a confirmatory step in IHC-defined MTAP-loss cases, this represents the positive predictive value of MTAP loss for CDKN2A homozygous deletion rather than a bidirectional concordance, and specificity was not formally assessed. Nonetheless, the result is consistent with the high specificity of MTAP IHC reported previously [15, 17], while occasional IHC/FISH discordance has also been described [16]. MTAP IHC, complemented by CDKN2A FISH where required, therefore provides a practical means of identifying this subgroup in routine practice.

This study has several limitations. First, this is a retrospective study based on tissue microarray analysis, which may not fully capture intra-tumoral heterogeneity despite the use of multiple cores per tumor. Second, although digital image analysis was used to quantify stromal and immune markers, the analyses relied on single-marker immunohistochemistry with threshold-based dichotomization, an established but less granular approach to fibroblast and immune phenotyping. Third, spatial relationships between tumor cells, stromal cells, and immune cells were not assessed in detail, and the lack of spatial or functional data precludes causal interpretation of the observed associations. Fourth, the diagnostic FISH analysis was performed only in MTAP-loss cases. Therefore, while our findings support the positive predictive value of MTAP loss for homozygous CDKN2A deletion, they do not permit formal assessment of sensitivity, specificity, or negative predictive value. Finally, survival analyses in subgroup cohorts should be interpreted with caution because of the limited subgroup sizes. Future studies integrating spatial transcriptomics, multiplex imaging, functional experiments, and extracellular-matrix proteomic profiling will be important to further define the biological consequences of MTAP loss in PDAC.

Conclusion

To our knowledge, this is among the first systematic characterizations of the stromal and immune microenvironment of MTAP-deficient PDAC. MTAP loss marks a distinct, myofibroblastic and selectively immune-attenuated tumor microenvironment, characterized by an SMA/FAP-high, PDGFRβ-low stromal marker profile and reduced NK-cell and plasma-cell infiltration, resembling an activated stromal state. This phenotype was not explained by basal-like tumor cell differentiation. As MTA-cooperative PRMT5 inhibitors advance in MTAP-deleted PDAC, these microenvironmental features should be considered in future translational studies and may inform rational combination and patient-selection strategies. MTAP

immunohistochemistry, complemented by CDKN2A FISH where required, offers a practical route to identifying this subgroup in routine diagnostic practice

Methods

Patient Cohort

This study included 370 patients with PDAC who underwent primary surgical resection within the prospective multicentric PANCALYZE study. Tumor samples were collected at the participating centers and processed centrally at the Institute of Pathology, University Hospital Cologne. Clinicopathological data (age, sex, grading, TNM stage) and overall survival (time from resection to death or last follow-up) were retrieved from pathology reports and clinical records. All cases were reviewed by experienced pathologists to confirm the diagnosis of PDAC according to WHO classification criteria.

Tissue Microarray Construction

A multi-spot tissue microarray (TMA) was constructed from formalin-fixed, paraffin-embedded (FFPE) tumor tissue. For each case, four representative tumor areas were selected and sampled using a tissue microarrayer as described before [28]. Each core measured 1.2 mm in diameter. The use of multiple cores per tumor was intended to account for intra-tumoral heterogeneity. TMA blocks were cut into 4 µm sections for immunohistochemical and FISH analyses.

Immunohistochemistry

As this study was part of the large cohort PANCALYZE study project, most staining protocols, antibody clones, and scoring cut-offs have already been described in the respective prior publications and are therefore only quickly summarized below. Detailed information can be found in Supplementary Table S2 (antibody list).

MTAP expression was assessed with the rabbit monoclonal antibody clone E5R1I (Cell Signaling Technology, Danvers, MA, USA; dilution 1:1000) and was conducted using the staining system Leica BOND-MAX with Leica Bond Polymer Refine Detection Kit (Leica Biosystems, Wetzlar, Germany). MTAP expression was scored in a binary manner as loss (complete absence of cytoplasmic tumor cell-staining with retained internal positive controls such as stroma or lymphocytes) or retained (any tumor-cell staining).

All immunohistochemical stainings were independently evaluated by pathologists (TB, SIL and AQ), who were blinded to clinical and molecular data.

Cell-type and immune markers (quantified as positive cells per sample by digital image analysis): CD163 (M2 macrophages), CD56 (NK cells), CD117 (mast cells), CD66b (tumor-associated neutrophils), CD20 (B cells), CD3 (T cells), CD38 (plasma cells). Cut-offs from our previous PANCALYZE analysis were CD3

high ≥ 110, CD38 high ≥ 15, and CD66b high ≥ 158 cells/sample [29]. CD20, CD56, CD117 and CD163 were dichotomized at the cohort median.

Stromal and CAF markers (SMA, FAP, PDGFRβ, periostin) were quantified by digital image analysis and dichotomized as described [30], with the cut-off set at the 45th percentile for SMA and at the median for FAP, PDGFRβ and periostin.

Tumor-subtype and molecular markers: Claudin 18.2 was scored per section and dichotomized as positive (≥ 2 + intensity in at least 75% of tumor cells) or negative [31]. CK6 and CK5/6 were scored on a three-tier scale (negative; low-positive; high-positive) by pathologists, according to previous studies by our group and others [26]. γH2AX was assessed by H-score [32], with high defined as an H-score ≥ 120 (cohort mean) [33]. XIAP was scored as binary negative versus positive [29]. HK2 was assessed by H-score [32] and dichotomized at the cohort median into low (< 100) and high (≥ 100) expression, following our esophageal-adenocarcinoma protocol [34].

To further profile MTAP-deficient tumors, an additional panel of immune, stromal, and tumor-cell markers (FOXP3, CD4, CD8, CD68, MUM1, BRG1, BRM, ERG, MCT, and Tenascin) was evaluated within the MTAP-deficient subgroup, dichotomized at the marker-specific median.

Digital Slide Acquisition and Image Analysis

All stained slides were scanned using Aperio GT 450 DX (Leica Biosystems, Wetzlar, Germany). For digital image analysis, the open-source software QuPath v0.6.0 (University of Edinburgh, Edinburgh, UK) was used as previously described [35]. Positive cells were quantified and marker densities calculated per core. The mean across the four cores per tumor was used for analysis. Cases with missing or non-evaluable cores were excluded from the respective marker analysis.

Fluorescence In Situ Hybridization (FISH)

CDKN2A FISH was performed to confirm the MTAP-deficient cases identified by IHC using a dual-color probe (ZytoLight SPEC CDKN2A/CEN9, ZytoVision, Bremerhaven, Germany) and scored as previously outlined [36]. Homozygous deletion was defined as complete loss of CDKN2A (green) signals with retained centromere-9 (orange) control signals. Signals were evaluated on a Leica DM5500 B fluorescence microscope (Leica Microsystems, Wetzlar, Germany) and imaging was performed with a JVC KY F75 digital camera (JVCKENWOOD USA Corporation, Long Beach, USA). In cases in which assessment on the TMA cores was equivocal, large-area whole sections for both MTAP IHC and CDKN2A FISH were re-ordered and re-evaluated (15 cases).

Statistical Analysis

The Chi-Square test was used for qualitative variables and age was dichotomized (< 65 vs. ≥ 65 years). Overall survival was analyzed using Kaplan–Meier curves and the log-rank test, both for the entire cohort (stratified by MTAP status) and within the MTAP-deficient subgroup. Univariable Cox regression analysis

was performed for all variables within the MTAP-deficient subgroup and only factors with $p < 0.20$ were entered into the multivariable Cox model. A p-value < 0.05 was considered significant. Statistical analyses were performed using IBM SPSS Statistics (Version 29.0.1.1, IBM, Armonk, USA).

Ethics approval

The study was approved by the Ethics Committee of the University Hospital Cologne (protocol number 25-1380). All experiments were performed in accordance with relevant guidelines and regulations, including the Declaration of Helsinki. Written informed consent was waived due to the retrospective nature of the study.

Use of large language models

Claude Opus 4.5, Claude Opus 4.6 and Claude Opus 4.8 (Anthropic, San Francisco, CA, USA), accessed via the Claude Code command-line interface, were used to improve the readability and language of the manuscript and to assist in writing code for data visualization. All AI-assisted output was reviewed and edited by the authors, who take full responsibility for the accuracy of the final manuscript.

Abbreviations

CAF
cancer-associated fibroblast
CDKN2A
cyclin-dependent kinase inhibitor 2A
CEP9
centromere enumeration probe, chromosome 9
CI
confidence interval
CK
cytokeratin
DAPI
4',6-diamidino-2-phenylindole
FAP
fibroblast activation protein
FFPE
formalin-fixed, paraffin-embedded
FISH
fluorescence in situ hybridization
FOXP3
forkhead box P3
γH2AX
histone H2AX phosphorylated at serine 139

HK2
hexokinase 2
HR
hazard ratio
IHC
immunohistochemistry
MTA
methylthioadenosine
MTAP
5'-methylthioadenosine phosphorylase
myCAF
myofibroblastic cancer-associated fibroblast
NK
natural killer
OS
overall survival
PDAC
pancreatic ductal adenocarcinoma
PDGFRβ
platelet-derived growth factor receptorβ
PRMT5
protein arginine methyltransferase 5
SMA (α-SMA)
α-smooth muscle actin
TMA
tissue microarray
TME
tumor microenvironment
TNM
tumor–node–metastasis
WHO
World Health Organization
XIAP
X-linked inhibitor of apoptosis protein

Declarations

Data Availability

The data supporting the findings of this study are available from the corresponding author upon reasonable request.

Consortium

The PANCALYZE Study Group: Felix C. Popp[2], Michael Heise[3], Frank Marusch[4], Marco Siech[5], Tawfik Mosa[6], Bodo Schniewind[7], Jürgen Tepel[8], Werner Hartwig[9], Christoph Prinz[10], Bettina M. Rau[11], Marco Niedergethmann[12], Rainer Kube[13], George Saada[14], Wolfgang Hiller[15] and Utz Settmacher[16]

[2] Department of General, Visceral, Thoracic and Transplantation Surgery, Faculty of Medicine and University Hospital of Cologne, Cologne, Germany

[3] Department of General and Visceral Surgery, Sana Klinikum Lichtenberg, Berlin, Germany

[4] Department of General and Visceral Surgery, Klinikum Ernst von Bergmann, Potsdam, Germany

[5] Department of General and Visceral Surgery, Ostalb-Klinikum Aalen, Aalen, Germany

[6] Department of General and Visceral Surgery, Carl-von-Basedow Klinikum Saalekreis, Merseburg, Germany

[7] Department of General and Visceral Surgery, Municipal Hospital Lüneburg, Lüneburg, Germany

[8] Department of General and Visceral Surgery, Klinikum Osnabrück, Osnabrück, Germany

[9] Department of General and Visceral Surgery, Evangelisches Krankenhaus Düsseldorf, Düsseldorf, Germany

[10] Department of General and Visceral Surgery, KMG Klinikum Güstrow, Güstrow, Germany

[11] Department of General and Visceral Surgery, Klinikum Neumarkt, Neumarkt, Germany

[12] Department of General and Visceral Surgery, Alfried Krupp Krankenhaus, Essen, Germany

[13] Department of General and Visceral Surgery, Carl-Thiem-Klinikum Cottbus, Cottbus, Germany

[14] Department of General and Visceral Surgery, Klinikum Robert Koch Gehrden, Gehrden, Germany

[15] Department of General and Visceral Surgery, Klinikum Lippe, Detmold, Germany

[16] Department of General and Visceral Surgery, University Hospital of Jena, Jena, Germany

Acknowledgements

We would like to thank the PANCALYZE study group investigators, who are listed in the Consortium section. The authors thank Wiebke Jeske for excellent technical assistance.

Funding

Open Access funding enabled and organized by Projekt DEAL. This research received no external funding.

Author Contributions

Karlbauer had full access to all the data in the study and takes responsibility for the integrity of the data and the accuracy of the data analysis.

Concept and design: Quaas, Bedau

Acquisition, analysis, or interpretation of data: All authors

Drafting of the manuscript: Quaas, Karlbauer, Knipper, Lyu

Critical revision of the manuscript for important intellectual content: Bruns, Buettner, Schloesser

Statistical analysis: Knipper

Supervision: Bruns, Buettner, Thomas

All authors reviewed and approved the final manuscript.

Additional Information

Competing interests

The authors declare no competing interests.

References

1. Arnold M, Abnet CC, Neale RE, et al. Global Burden of 5 Major Types of Gastrointestinal Cancer. *Gastroenterology*. 2020;159(1):335-349.e15. doi:10.1053/j.gastro.2020.02.068
2. Hu JX, Zhao CF, Chen WB, et al. Pancreatic cancer: A review of epidemiology, trend, and risk factors. *World J Gastroenterol*. 2021;27(27):4298-4321. doi:10.3748/wjg.v27.i27.4298
3. Waddell N, Pajic M, Patch AM, et al. Whole genomes redefine the mutational landscape of pancreatic cancer. *Nature*. 2015;518(7540):495-501. doi:10.1038/nature14169
4. Wu C, Yang P, Liu B, Tang Y. Is there a CDKN2A-centric network in pancreatic ductal adenocarcinoma? *OncoTargets Ther*. 2020;13:2551-2562. doi:10.2147/OTT.S232464
5. Bray C, Balcells C, McNeish IA, Keun HC. The potential and challenges of targeting MTAP-negative cancers beyond synthetic lethality. *Front Oncol*. 2023;13:1264785. doi:10.3389/fonc.2023.1264785
6. Vrugt B, Kirschner MB, Meerang M, et al. Deletions of CDKN2A and MTAP Detected by Copy-Number Variation Array Are Associated with Loss of p16 and MTAP Protein in Pleural Mesothelioma. *Cancers*. 2023;15(20):4978. doi:10.3390/cancers15204978

7. Kryukov GV, Wilson FH, Ruth JR, et al. MTAP deletion confers enhanced dependency on the arginine methyltransferase PRMT5 in human cancer cells. *Science*. 2016;351(6278):1214-1218. doi:10.1126/science.aad5214
8. Stopa N, Krebs JE, Shechter D. The PRMT5 arginine methyltransferase: many roles in development, cancer and beyond. *Cell Mol Life Sci*. 2015;72(11):2041-2059. doi:10.1007/s00018-015-1847-9
9. Hu M, Chen X. A review of the known MTA-cooperative PRMT5 inhibitors. *RSC Adv*. 2024;14(53):39653-39691. doi:10.1039/D4RA05497K
10. Schneider C, Spielmann V, Braun CJ, Schneider G. PRMT5 inhibitors: Therapeutic potential in pancreatic cancer. *Transl Oncol*. 2025;55:102366. doi:10.1016/j.tranon.2025.102366
11. Engstrom LD, Aranda R, Waters L, et al. MRTX1719 Is an MTA-Cooperative PRMT5 Inhibitor That Exhibits Synthetic Lethality in Preclinical Models and Patients with MTAP-Deleted Cancer. *Cancer Discov*. 2023;13(11):2412-2431. doi:10.1158/2159-8290.CD-23-0669
12. Pant S, Ducreux MP, Ikeda M, et al. A phase 2/3 randomized study of BMS-986504 with nab-paclitaxel (nab-P) and gemcitabine (GEM) in first-line (1L) metastatic pancreatic ductal adenocarcinoma (PDAC) with homozygous *MTAP* deletion (*MTAP*-del): MountainTAP-30. *J Clin Oncol*. 2026;44(2_suppl). doi:10.1200/JCO.2026.44.2_suppl.TPS796
13. Maragkou T, Reinhard S, Jungo P, et al. Evaluation of MTAP and p16 immunohistochemical deficiency as surrogate marker for CDKN2A/B homozygous deletion in gliomas. *Pathology*. 2023;55(4):466-477. doi:10.1016/j.pathol.2023.01.005
14. Dono A, Pichardo-Rojas D, Mendoza Mora L, et al. MTAP immunohistochemistry as a surrogate marker of CDKN2A loss in brain tumors: A meta-analysis and literature review. *J Neuropathol Exp Neurol*. 2025;84(7):600-610. doi:10.1093/jnen/nlaf033
15. Gorbokon N, Teljuk K, Reiswich V, et al. Deficiency of MTAP Is Frequent and Mostly Homogeneous in Pancreatic Ductal Adenocarcinomas. *Cancers*. 2025;17(7):1205. doi:10.3390/cancers17071205
16. Lucà S, Salzillo C, Masola V, et al. MTAP in small biopsy samples of pancreatic lesions: a potential diagnostic biomarker. Immunohistochemical, fluorescence in situ hybridization and molecular analysis. *Pathologica*. 2025;117(5):486-495. doi:10.32074/1591-951X-1243
17. Lyu SI, Knipper K, Fretter C, et al. MTAP loss in gastrointestinal cancers is associated with CDKN2A deletion, poor prognosis in gastric carcinoma, and potential relevance for PRMT5-targeted therapy. *Sci Rep*. 2026;16(1):15061. doi:10.1038/s41598-026-51370-9
18. Kalluri R. The biology and function of fibroblasts in cancer. *Nat Rev Cancer*. 2016;16(9):582-598. doi:10.1038/nrc.2016.73
19. Öhlund D, Handly-Santana A, Biffi G, et al. Distinct populations of inflammatory fibroblasts and myofibroblasts in pancreatic cancer. *J Exp Med*. 2017;214(3):579-596. doi:10.1084/jem.20162024
20. Biffi G, Tuveson DA. Diversity and Biology of Cancer-Associated Fibroblasts. *Physiol Rev*. 2021;101(1):147-176. doi:10.1152/physrev.00048.2019
21. Steele NG, Carpenter ES, Kemp SB, et al. Multimodal Mapping of the Tumor and Peripheral Blood Immune Landscape in Human Pancreatic Cancer. *Nat Cancer*. 2020;1(11):1097-1112.

doi:10.1038/s43018-020-00121-4

22. Han G, Yang G, Hao D, et al. 9p21 loss confers a cold tumor immune microenvironment and primary resistance to immune checkpoint therapy. *Nat Commun*. 2021;12(1):5606. doi:10.1038/s41467-021-25894-9
23. Gjuka D, Adib E, Garrison K, et al. Enzyme-mediated depletion of methylthioadenosine restores T cell function in MTAP deficient tumors and reverses immunotherapy resistance. *Cancer Cell*. 2023;41(10):1774-1787.e9. doi:10.1016/j.ccell.2023.09.005
24. Sahin U, Koslowski M, Dhaene K, et al. Claudin-18 Splice Variant 2 Is a Pan-Cancer Target Suitable for Therapeutic Antibody Development. *Clin Cancer Res*. 2008;14(23):7624-7634. doi:10.1158/1078-0432.CCR-08-1547
25. Mah LJ, El-Osta A, Karagiannis TC. γH2AX: a sensitive molecular marker of DNA damage and repair. *Leukemia*. 2010;24(4):679-686. doi:10.1038/leu.2010.6
26. Lyu SI, Krey T, Damanakis AI, et al. Cytokeratin 6 identifies basal-like subtypes of pancreatic ductal adenocarcinoma with decreased survival. *J Cancer Res Clin Oncol*. 2023;149(10):7539-7546. doi:10.1007/s00432-023-04702-5
27. Bailey P, Chang DK, Nones K, et al. Genomic analyses identify molecular subtypes of pancreatic cancer. *Nature*. 2016;531(7592):47-52. doi:10.1038/nature16965
28. Quaas A, Pamuk A, Klein S, et al. Sex-specific prognostic effect of CD66b-positive tumor-infiltrating neutrophils (TANs) in gastric and esophageal adenocarcinoma. *Gastric Cancer*. 2021;24(6):1213-1226. doi:10.1007/s10120-021-01197-2
29. Knipper K, Lyu SI, Goebel H, et al. X-linked inhibitor of apoptosis protein is a prognostic marker for a favorable outcome in three identified subsets in resectable adenocarcinoma of the pancreas. *J Cancer Res Clin Oncol*. 2023;149(9):5531-5538. doi:10.1007/s00432-022-04476-2
30. Knipper K, Damanakis AI, Zhao Y, et al. Specific Subtypes of Carcinoma-Associated Fibroblasts Are Correlated with Worse Survival in Resectable Pancreatic Ductal Adenocarcinoma. *Cancers*. 2023;15(7):2049. doi:10.3390/cancers15072049
31. Lyu SI, Fretter C, Simon AG, et al. Extent and clinical significance of the therapy-relevant tight junction protein Claudin 18.2 in pancreatic ductal adenocarcinoma - real-world evidence. *Transl Oncol*. 2024;47:102044. doi:10.1016/j.tranon.2024.102044
32. Mazières J, Brugger W, Cappuzzo F, et al. Evaluation of EGFR protein expression by immunohistochemistry using H-score and the magnification rule: Re-analysis of the SATURN study. *Lung Cancer*. 2013;82(2):231-237. doi:10.1016/j.lungcan.2013.07.016
33. Knipper K, Hussein Y, Simon AG, et al. Upregulation of the histone γ-H2AX correlates with worse patient survival and basal-like subtype in pancreatic ductal adenocarcinoma. *J Cancer Res Clin Oncol*. 2024;150(3):137. doi:10.1007/s00432-024-05681-x
34. Lyu SI, Simon AG, Jung JO, et al. Hexokinase 2 as an independent risk factor for worse patient survival in esophageal adenocarcinoma and as a potential therapeutic target protein: A retrospective, single-center cohort study. *Oncol Lett*. 2024;28(4):495. doi:10.3892/ol.2024.14628

35. Bankhead P, Loughrey MB, Fernández JA, et al. QuPath: Open source software for digital pathology image analysis. *Sci Rep*. 2017;7:16878. doi:10.1038/s41598-017-17204-5
36. Schildhaus HU, Heukamp LC, Merkelbach-Bruse S, et al. Definition of a fluorescence in-situ hybridization score identifies high- and low-level FGFR1 amplification types in squamous cell lung cancer. *Mod Pathol*. 2012;25(11):1473-1480. doi:10.1038/modpathol.2012.102
37. Puleo F, Nicolle R, Blum Y, et al. Stratification of Pancreatic Ductal Adenocarcinomas Based on Tumor and Microenvironment Features. *Gastroenterology*. 2018;155(6):1999-2013.e3. doi:10.1053/j.gastro.2018.08.033
38. Bady E, Müller JH, Simon R, et al. Abstract 7404: MTAP loss reshapes the immune and proliferative landscape of pancreatic ductal adenocarcinoma. *Cancer Res*. 2026;86(7_Supplement):7404. doi:10.1158/1538-7445.AM2026-7404
39. Gong J, Ciombor K, Valerin J, et al. Characterization of the tumor immune microenvironment (TIME) and somatic landscape in gastrointestinal (GI) malignancies with MTAP deletions (del). *J Clin Oncol*. 2025;43:835. doi:10.1200/JCO.2025.43.4_suppl.835
40. Veghini L, Pasini D, Fang R, et al. Differential activity of MAPK signalling defines fibroblast subtypes in pancreatic cancer. *Nat Commun*. 2024;15:10534. doi:10.1038/s41467-024-54975-8
41. Moffitt RA, Marayati R, Flate EL, et al. Virtual microdissection identifies distinct tumor- and stroma-specific subtypes of pancreatic ductal adenocarcinoma. *Nat Genet*. 2015;47(10):1168-1178. doi:10.1038/ng.3398
42. Robertson FP, Cameron A, Spiers HVM, et al. Evidence for molecular subtyping in pancreatic ductal adenocarcinoma: a systematic review. *HPB*. 2024;26(5):609-617. doi:10.1016/j.hpb.2024.02.001
43. Ngoi NYL, Tang TY, Gaspar CF, et al. Methylthioadenosine Phosphorylase Genomic Loss in Advanced Gastrointestinal Cancers. *Oncologist*. 2024;29(6):493-503. doi:10.1093/oncolo/oyae011
44. Mauri G, Patelli G, Roazzi L, et al. Clinicopathological characterisation of MTAP alterations in gastrointestinal cancers. *J Clin Pathol*. 2025;78(3):195-201. doi:10.1136/jcp-2023-209341
45. Hu H, Hang JJ, Han T, Zhuo M, Jiao F, Wang LW. The M2 phenotype of tumor-associated macrophages in the stroma confers a poor prognosis in pancreatic cancer. *Tumour Biol*. 2016;37(7):8657-8664. doi:10.1007/s13277-015-4741-z
46. Rodon J, Johnson ML, George B, Shah PA, Arbour KC. MTAP Deletion in Oncogenesis: A Synthetic Lethality Scenario. *Cancer Res*. 2026;86(7):1558-1569. doi:10.1158/0008-5472.CAN-25-2126
47. Bristol-Myers Squibb. *A Randomized, Phase 2/3 Study Comparing Navlimetostat (BMS-986504) in Combination With Nab-Paclitaxel and Gemcitabine Versus Placebo in Combination With Nab-Paclitaxel and Gemcitabine in Participants With Untreated Metastatic Pancreatic Ductal Adenocarcinoma Harboring Homozygous MTAP Deletion*. clinicaltrials.gov; 2026. Accessed July 3, 2026. https://clinicaltrials.gov/study/NCT07076121
48. Bristol-Myers Squibb. *A Multicenter, Randomized, Open-Label, Phase 2 Study Evaluating the Safety and Efficacy of Navlimetostat (BMS-986504) Monotherapy in Participants With Advanced or Metastatic Non-Small Cell Lung Cancer (NSCLC) With Homozygous MTAP Deletion After Progression on Prior*

Therapies. clinicaltrials.gov; 2026. Accessed July 3, 2026. https://clinicaltrials.gov/study/NCT06855771

49. Drizyte-Miller K, Engstrom LD, Klomp JA, et al. Combination of the MTA-Cooperative PRMT5 Inhibitor BMS-986504 and KRAS Inhibitors is an Effective Treatment Strategy for MTAP-Deleted KRAS-Mutant Pancreatic Cancer. *Cancer Res*. 2025;85(18):3540-3557. doi:10.1158/0008-5472.CAN-25-1507
50. Henriksen A, Dyhl-Polk A, Chen I, Nielsen D. Checkpoint inhibitors in pancreatic cancer. *Cancer Treat Rev*. 2019;78:17-30. doi:10.1016/j.ctrv.2019.06.005

Tables

Table 1. General clinicopathological values of the total study population and patients with MTAP loss versus retained MTAP. G: grading, L: lymphatic infiltration, Pn: perineural infiltration, pN: pathological lymph node status, pT: pathological tumor status, R: resection status, V: blood invasion. Bold p-values mark statistical significance.

Characteristic	Total	MTAP		p-value
		Loss	Retained	
	n (%)	n (%)	n (%)	
No. of patients	370 (100)	146 (39.5)	224 (60.5)	
Age				
Under 65	128 (34.6)	62 (42.5)	66 (29.5)	**0.010**
65 and above	242 (65.4)	84 (57.5)	158 (70.5)	
Sex				
Male	183 (49.5)	76 (52.1)	107 (47.8)	0.420
Female	187 (50.5)	70 (47.9)	117 (52.2)	
Neoadjuvant therapy				
No	346 (94.3)	134 (93.7)	212 (94.6)	0.871
Chemotherapy	18 (4.9)	8 (5.6)	10 (4.5)	
Radiochemotherapy	3 (0.8)	1 (0.7)	2 (0.9)	
pT				
0	1 (0.3)	1 (0.7)	0 (0.0)	0.630
1	26 (7.0)	9 (6.2)	17 (7.6)	
2	145 (39.2)	59 (40.4)	86 (38.4)	
3	190 (51.4)	75 (51.4)	115 (51.3)	
4	8 (2.2)	2 (1.4)	6 (2.7)	
pN				
0	104 (28.1)	40 (27.4)	64 (28.6)	**0.045**
1	262 (70.8)	102 (69.9)	160 (71.4)	
2	4 (1.1)	4 (2.7)	0 (0.0)	
R				
0	247 (66.8)	93 (63.7)	154 (68.8)	0.590
1	121 (32.7)	52 (35.6)	69 (30.8)	
2	2 (0.5)	1 (0.7)	1 (0.4)	
L				

Characteristic	Total	MTAP		p-value
		Loss	Retained	
	n (%)	n (%)	n (%)	
0	146 (39.9)	58 (40.3)	88 (39.6)	0.903
1	220 (60.1)	86 (59.7)	134 (60.4)	
V				
0	256 (70.5)	102 (71.3)	154 (70.0)	0.707
1	106 (29.2)	41 (28.7)	65 (29.5)	
Unknown	1 (0.3)	0 (0.0)	1 (0.5)	
Pn				
0	90 (25.2)	32 (22.2)	58 (27.2)	0.285
1	267 (74.8)	112 (77.8)	155 (72.8)	
G				
0	9 (2.5)	3 (2.1)	6 (2.8)	0.211
1	10 (2.8)	1 (0.7)	9 (4.2)	
2	181 (50.4)	78 (54.5)	103 (47.7)	
3	156 (43.5)	59 (41.3)	97 (44.9)	
4	3 (0.8)	2 (1.4)	1 (0.5)	

Table 2. Overall survival analysis within the MTAP-deficient subgroup. Median overall survival is shown in months with 95% confidence intervals. P-values were calculated using the log-rank test. Case numbers differ between markers due to marker-specific tissue availability and evaluability on the tissue microarray. Bold p-values mark statistical significance.

Marker	Group	n (events)	Median OS, months (95% CI)	p-value
FOXP3	Low	72 (53)	17.0 (13.1–20.9)	0.054
	High	72 (41)	26.0 (21.7–30.3)	
Claudin 18.2	Negative	58 (43)	15.0 (10.1–19.9)	**0.025**
	Positive	33 (21)	30.0 (26.2–33.8)	
γH2AX	Low	49 (29)	26.0 (22.1–29.9)	**0.003**
	High	41 (33)	14.0 (9.3–18.7)	
CD163	Low	70 (41)	26.0 (21.3–30.7)	**0.007**
	High	75 (53)	18.0 (12.6–23.4)	

Table 3. Multivariable Cox regression within the MTAP-deficient subgroup.

Characteristic	Hazard Ratio	95% CI	p
Age (<65 vs ≥65)	0.60	0.35–1.04	0.070
Neoadjuvant therapy	2.06	0.65–6.48	0.218
pT	1.44	0.84–2.46	0.184
pN	1.58	0.82–3.03	0.170
R category	0.86	0.47–1.56	0.612
Blood invasion	1.75	0.92–3.33	0.088
γH2AX (high vs low)	1.97	1.08–3.62	**0.028**
CD163 (high vs low)	1.42	0.78–2.57	0.251
FAP (high vs low)	1.75	0.96–3.20	0.069
FOXP3 (high vs low)	0.60	0.33–1.10	0.097

HR, hazard ratio; CI, confidence interval. Only factors with p < 0.20 in univariable Cox regression were entered into the multivariable model. Bold p-values mark statistical significance.

Figures

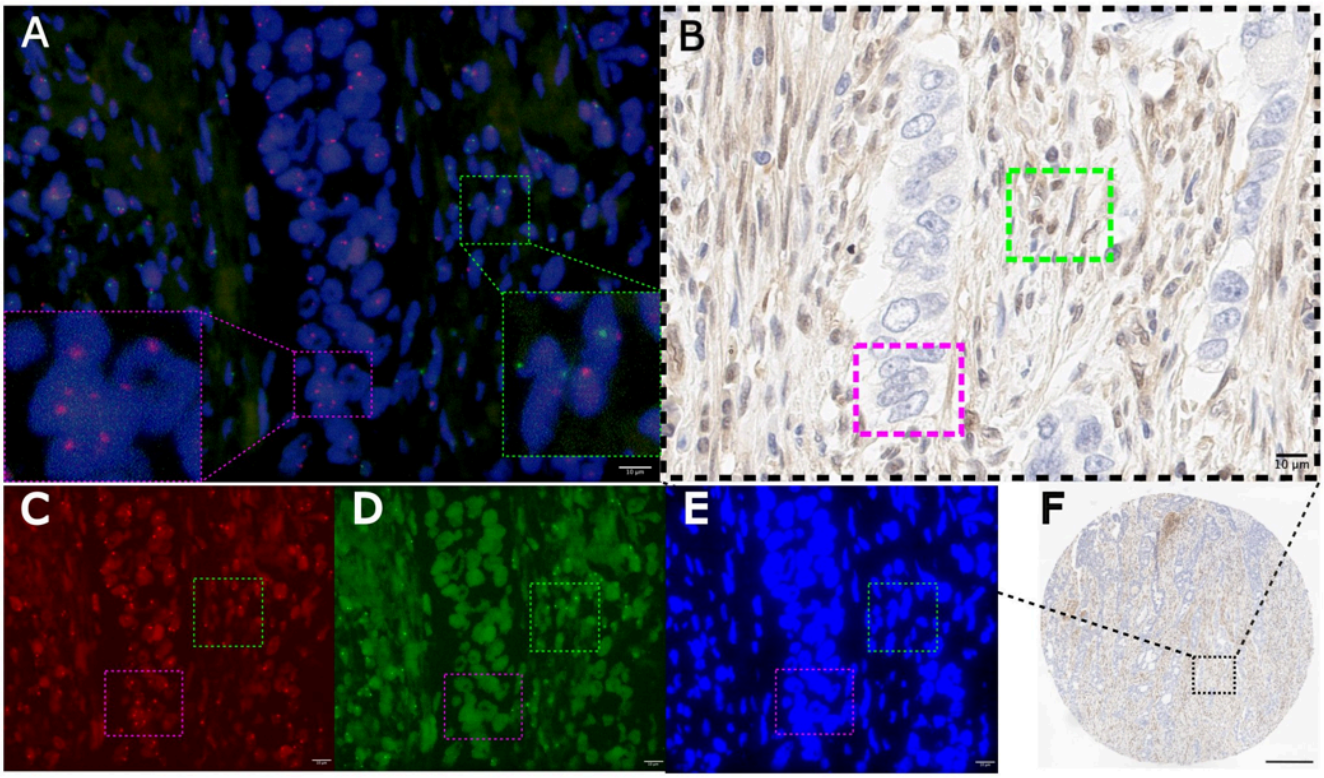


Figure 1

MTAP loss corresponds to homozygous CDKN2A (9p21) deletion. Matched MTAP IHC and CDKN2A FISH on adjacent serial sections. **(A)** Merged CDKN2A FISH showing CDKN2A (green), CEP9 (orange), and DAPI (blue). Tumor (pink box): homozygous CDKN2A deletion (loss of green, retained orange). Stroma (green box): retained CDKN2A. Insets show representative nuclei with intact and deleted CDKN2A. **(B)**Corresponding MTAP IHC showing MTAP loss in tumor gland (pink box) and retained expression in stroma (green box). **(C–E)** Individual FISH channels: **(C)**CEP9, **(D)** CDKN2A, **(E)** DAPI. **(F)** Low-power overview of the corresponding TMA core. Boxed area shown in A–E. Scale bars: 10 μm (A–E) and 200 μm (F).

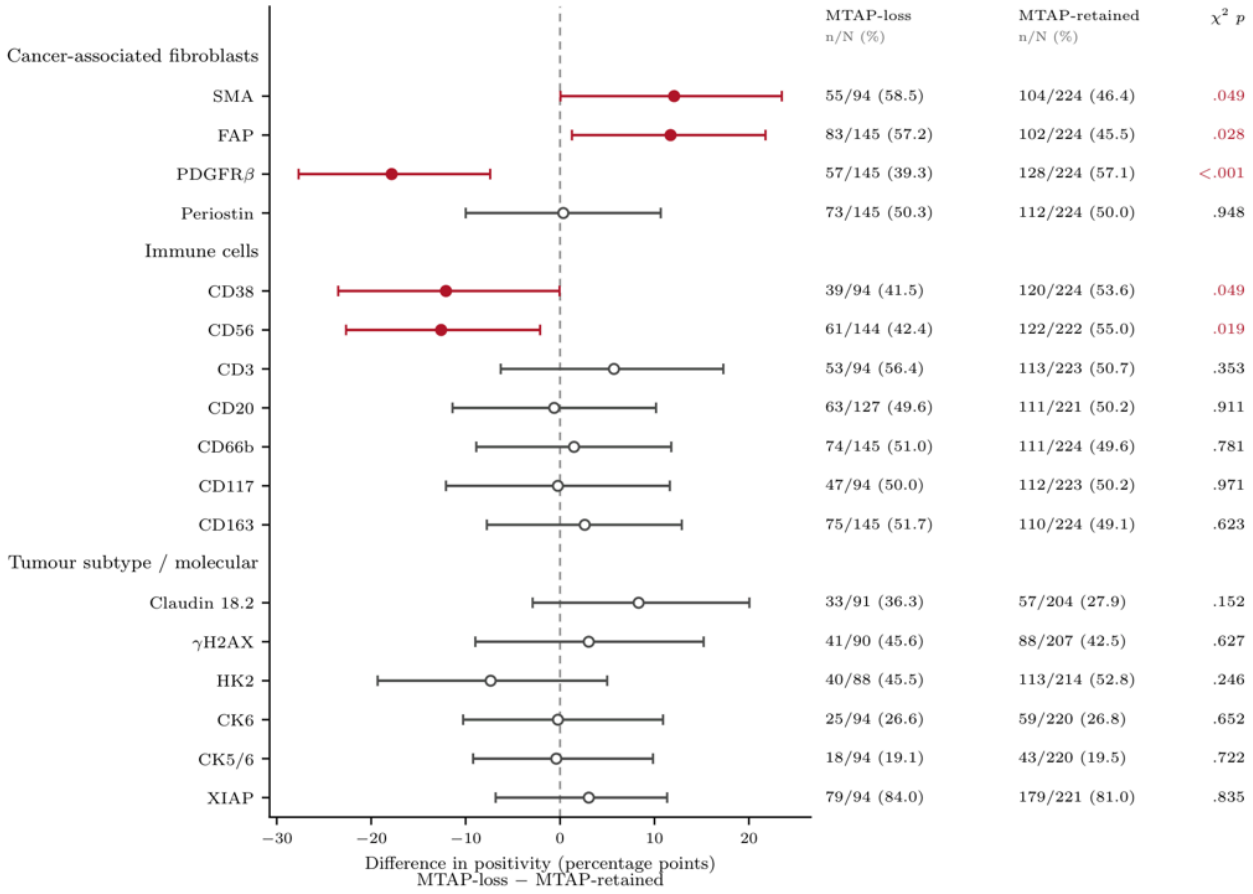


Figure 2

TME markers by MTAP status in PDAC. Points show the difference in the proportion of positive cases (MTAP-loss minus MTAP-retained, percentage points). Horizontal bars are 95% Newcombe confidence intervals. P-values are the Pearson χ^2 tests from the original analysis (red: $p < 0.05$). For ordinally scored markers the plotted proportion is dichotomized for display — CK6/CK5/6, score 2; XIAP, scores 1–3 vs 0. For these three markers the confidence interval refers to this dichotomized proportion, whereas their p-value refers to the full ordinal distribution as originally tested. All three are non-significant under either definition. n/N, positive/evaluable cases.

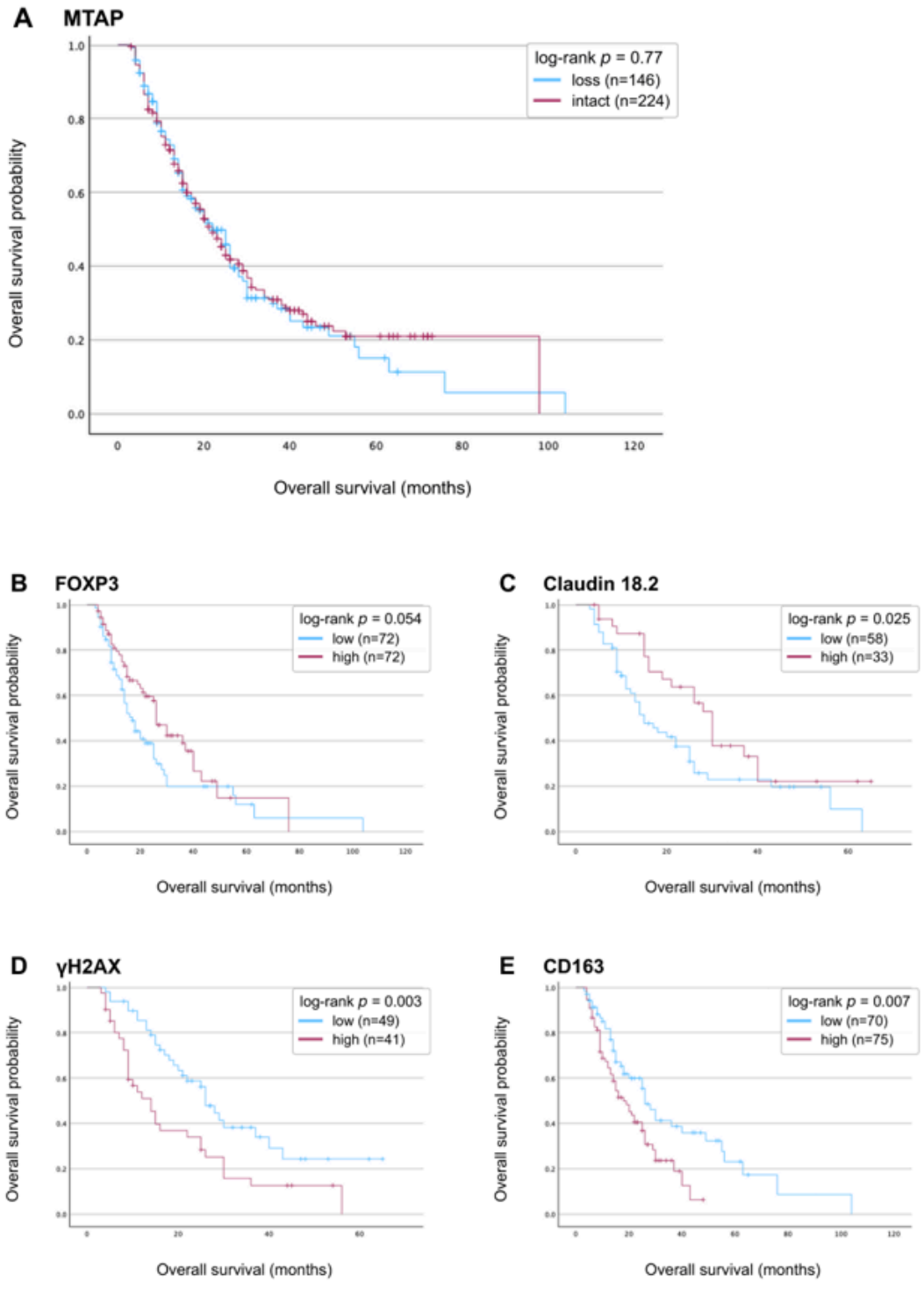


Figure 3

Kaplan–Meier overall survival. (A) Whole cohort by MTAP status (loss vs. intact; n = 370). No significant difference (log-rank p = 0.77). (B–E) Within MTAP-deficient PDAC, stratified by FOXP3 (B), Claudin 18.2 (C), γH2AX (D), and CD163 (E).

Supplementary Files

This is a list of supplementary files associated with this preprint. Click to download.

- SupplementaryInformation.pdf